Interface reconstruction of $MSi_2/Si(001)$ (M=Co,Ni) from first principles

F. F. Zhao, Y. P. Feng,* Y. F. Dong, and J. Z. Zheng
Department of Physics, National University of Singapore, 2 Science Drive 3, Singapore 117542
(Received 14 January 2006; revised manuscript received 13 March 2006; published 5 July 2006)

First-principles calculations based on density-functional theory and generalized gradient approximation were performed to study the interface structures of epitaxial $NiSi_2$ and $CoSi_2$ on a Si(001) substrate. A sevenfold-*Z* model with zigzag Si-dimer rows in the interface layer is proposed. The model is energetically comparable to an established sevenfold-*R* model and they could coexist in both $CoSi_2/Si$ and $NiSi_2/Si$ structures, leading possibly to degradation of the interface quality of the silicide/silicon heterostructure.

DOI: 10.1103/PhysRevB.74.033301 PACS number(s): 61.50.Ah, 68.35.Ct, 71.20.Be

Transition-metal silicides have been used in source/drain and polygate regions of ultra-high-speed complementary metal-oxide-semiconductor (CMOS) devices for a couple of decades due to their easy formation, good adhesion, and low resistivity. By forming a uniform and stable silicide thin film on top of a Si substrate, contact and interconnect resistances can be reduced, resulting in a decreasing RC delay time and improvement of device performance. Among various kinds of silicides, $CoSi_2$ has been widely used in 0.18 μm to 65 nm technology nodes for ultra-large-scale integration (ULSI). $NiSi_2$ has the same cubic calcium fluoride CaF_2 structure (space group $Fm\bar{3}m$) as $CoSi_2$, where each Si atom has four metal (*M*) neighbors forming a tetrahedron and eight Si atoms sit around each *M* atom forming a cube. Compared to $CoSi_2$ (resistivity 18–20 $\mu\Omega$ cm), $NiSi_2$ has relatively higher resistivity ($\sim$50 $\mu\Omega$ cm) which is not desirable for CMOS devices. However, the lattice constant mismatch between $NiSi_2$ and Si is only 0.44%, which is even smaller than that between $CoSi_2$ and Si (1.22%). Therefore both $CoSi_2$ and $NiSi_2$ have attracted great attention and have been extensively studied both experimentally and theoretically.

Besides intrinsic electrical and mechanical properties of the bulk materials, interface structure and quality are of crucial importance for transport properties. Due to the small lattice mismatch, high quality epitaxial MSi_2 thin film can be grown on crystalline Si substrate. The epitaxial growth of $NiSi_2$ on (111), (110), and (100) surfaces of Si was first achieved in 1974 by Tu and co-workers.[1] Results of high-resolution transmission electron microscopy (HRTEM) showed an atomically flat interface, even though part of the $NiSi_2$(111) hexagonal basal plane is twinned with respect to the substrate orientation.[2–4] The films were found rotated by 180° about the normal of the Si surface (type-*B* orientation), as opposed to the original direction (type-*A* orientation). Unlike the mixture of type-*A* and type-*B* orientations for a $NiSi_2/Si(111)$ interface, only the type-*B* orientation with 180° twinning was observed for the epitaxial growth of $CoSi_2$ on Si(111).[5,6]

MSi_2 growth on top of a Si(001) surface is more complex than other surfaces in terms of atomic structure. Commonly the coordination of the interface metal atom is used to represent interfacial structure models. Two straightforward interface structures, the sixfold model and the eightfold model, were proposed by Cherns *et al.*[7] These models were constructed based on bulk-terminated Si and MSi_2 surfaces and allow optimal coordination for either Si or metal (*M*) atoms. In the sixfold configuration, each Si atom has four tetrahedral neighbors and the *M* atoms are sixfold-coordinated at the interface plane. While in the eightfold model, the *M* atoms are eightfold-coordinated as in the bulk. This results in some interface Si atoms with two dangling bonds. Recently, Yu *et al.* proposed a sevenfold model (sevenfold *U*),[8] in which each *M* atom has seven neighboring silicon atoms. In this model, Si atoms in the first layer next to the metal layer have four bonds within one plane rather than the tetrahedral structure, and Si atoms in the second layer form a normal tetrahedral configuration and one extra bond with the *M* atom. Besides the unreconstructed configurations, (2×1) reconstructed structures were observed by HRTEM at $CoSi_2/Si(001)$ interfaces and different models have been proposed based on the observations, such as the Loretto, Gibson, and Yalisove (LGY) model,[9] the Bulle-Lieuwma, de Jong, and Vandenhoudt (BJV) model,[10] and the sevenfold-*R* model by Yu *et al.*[8] The LGY model is a modification of the eightfold model by forming dimers between the interface Si atoms with two dangling bonds. The BJV model is based on the sevenfold-*U* model, an additional Si atom is inserted into the first Si interface plane and each of the inserted Si has two dangling bonds. To reduce the system energy, the interface Si atoms with four bonds in the sevenfold-*U* model were reconstructed as rows of dimers, which leads to the sevenfold-*R* model [Fig. 1(a)]. Previous studies predicted that the sevenfold-*R* model has the lowest energy compared to all of the other models, while the LGY, BJV, and the original sevenfold-*U* models are energetically unfavorable.[8] Interface structure with sevenfold (2×1) reconstruction was recently observed at $NiSi_2/Si(001)$ interfaces by scanning transmission electron microscopy (STEM).[11] The sevenfold-*R* structure was thus adopted as the model for the reconstructed $MSi_2/Si(001)$ interface.

While the sevenfold-*R* model is generally accepted, it fails to give a satisfactory explanation to the blurred Si dimer in the STEM image. A possible cause for the blurred image could be due to a shift of the Si dimers. It is known that in a clean Si(001) surface, Si atoms form buckled dimer rows to lower surface energy. However, whether such an argument is valid in an interface structure is questionable. Besides simple straight rows, it may be possible for the Si dimers to form zigzag rows, or other patterns. As a matter of fact, results of Monte Carlo simulation indicated that both "stripe" and

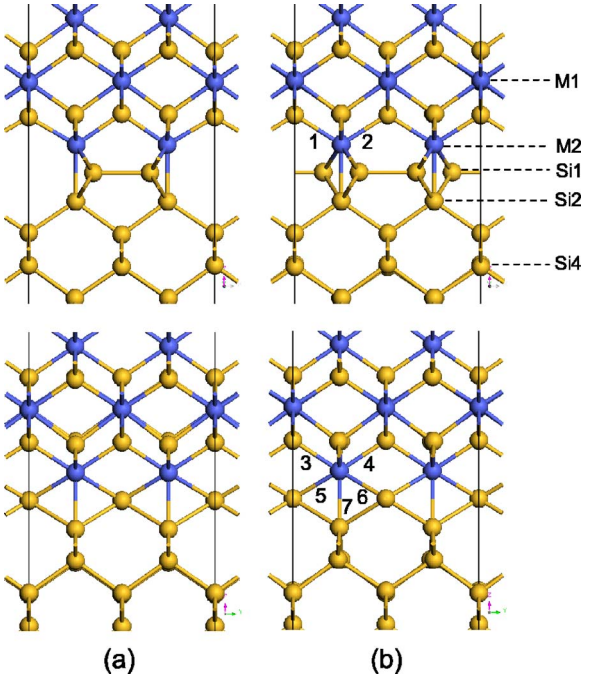

FIG. 1. (Color online) Structures of (a) sevenfold-*R* and (b) sevenfold-*Z* interfaces viewed in ⟨110⟩ (top) and ⟨1$\bar{1}$0⟩ (bottom) directions, respectively. Si atoms are shown by the yellow/light balls while metal atoms are represented by the blue/dark balls.

"check" patterns of fully bridge-bonded structures can exist simultaneously in a SiO_2/Si(001) interface.[12] Therefore, it would be useful and important to explore interface structures formed with different reconstructions. Motivated by this, we propose a reconstructed structure for the MSi_2/Si(001) interface. Named sevenfold *Z*, the interface model consists of zigzag Si dimer rows along the Si ⟨111⟩ direction at the interface [see Fig. 1(b)], in contrast to the straight Si dimer rows in the sevenfold-*R* model [Fig. 1(a)]. The structural stability and properties of the sevenfold-*Z* model are investigated here and compared with those of the sixfold, eightfold, and sevenfold-*R* models.

First-principles calculations based on the density-functional theory (DFT)[13] were performed by using a Vienna *ab initio* simulation package (VASP),[14] with Vanderbilt ultrasoft pseudopotentials[15] for electron-ion interactions and the generalized gradient approximation (GGA)[16] for the exchange-correlation potential between electrons. To determine the interface properties, a supercell scheme with two equivalent interfaces were adopted in our calculations. The supercell consisted of a 2×2 unit in the interface plane, and 13 MSi_2 atomic layers and 15 Si atomic layers in the interface normal direction to ensure that bulk Si and MSi_2 can be reproduced in regions away from the interface and the interaction between the two interfaces is negligible. A 6×6×5 *k*-point mesh generated according to the Monkhorst-Pack scheme[17] was used for tetragonal Si and MSi_2 cells. For the interface supercell containing 108 Si atoms and 28 M atoms, a 3×3×1 mesh was used during geometry relaxation of the various structures, and a 6×6×1 mesh for the energy calculation. The plane-wave basis set was truncated at an energy of 300 eV. The total energy difference of the supercell is less than 0.12 eV when the cutoff energy increased from 300 to 350 eV, showing good convergence and accuracy.

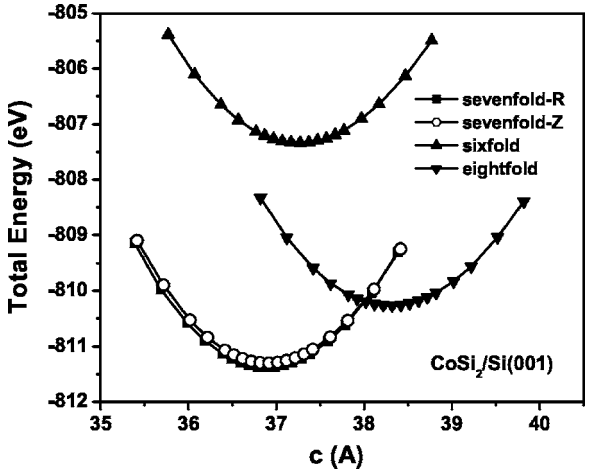

FIG. 2. Calculated total energy as a function of lattice parameter *c*, for the four interface models with 13 atomic layers of $CoSi_2$ and 15 atomic layers of Si each.

Structural optimization was carried out to determine the equilibrium interface structure. To simulate the growth of MSi_2 on a Si substrate, the lattice constants (*a* and *b*) in the plane parallel to the interface were fixed to the GGA optimized Si lattice constant of 5.456 Å, which is 0.46% larger than the experimental value of 5.431 Å.[18] The lattice parameter *c* is the periodic length of the supercell perpendicular to the interface plane, and its value reflects variations of the atomic distance and bonding length induced by different interface configurations. In our calculation, *c* was varied by up to 10% near the optimal value in steps and ionic relaxation was performed accordingly to reduce the total energy of $NiSi_2$/Si(001) and $CoSi_2$/Si(001) at each *c* value. Figure 2 shows the total energy as a function of *c* for the $CoSi_2$/Si(001) interface. By fitting the *E*-*V* data to the third-order Birch-Murnaghan equation of states,[19] the equilibrium lattice constant *c* of the various interface structures of the two silicides/silicon systems is determined and listed in Table I. It is clear that the two sevenfold models have much lower total energies and smaller *c* values compared to the sixfold and eightfold models. The eightfold model has a larger *c* because the Si atoms with dangling bonds tend to

TABLE I. Optimized lattice parameter *c* (Å) and calculated interface formation energy of different interface structures, relative to that of the sevenfold-*R* model, ΔE_{form}. Results from a previous study (Ref. 8) are shown in brackets.

	c (Å)		ΔE_{form} (eV/2×1)	
Model	$NiSi_2$/Si	$CoSi_2$/Si	$NiSi_2$/Si	$CoSi_2$/Si
Sixfold	37.810	37.257	0.566 (0.42)	1.010 (0.87)
Eightfold	38.987	38.301	1.797 (1.74)	0.278 (0.27)
Sevenfold –*R*	37.328	36.884	0 (0)	0 (0)
Sevenfold -*Z*	37.371	36.906	−0.017	0.019

push the next Si layer away. For example, in the $CoSi_2$/Si(001) system, the bond length between two Si atoms in the first layer and the second layer, respectively, is 2.347 Å in the sixfold configuration while it is 2.461 Å in the eightfold structure.

To evaluate the relative stability of the interfaces, interface formation energy E_{form} is estimated from $E_{form}=[E_{tot}-(n\mu_{MSi_2}+m\mu_{Si})]/(2A)$, where E_{tot} is the DFT total energy of the interface supercell, n and m are the numbers of MSi_2 and Si bulk units in the supercell respectively, μ_{MSi_2} and μ_{Si} are the chemical potentials of MSi_2 and Si, respectively, and A is the interface area. The factor of 2 accounts for the two identical interfaces in the supercell. For simplicity, it is assumed that the interface structures are in thermal equilibrium with bulk Si and bulk MSi_2. Thus the chemical potentials, μ_{MSi_2} and μ_{Si}, can be replaced by the corresponding DFT total energies of the bulk units, E_{MSi_2} and E_{Si}, respectively. The calculated interface formation energies are 29 meV/Å^2 and 62 meV/Å^2 for the sevenfold-Z $NiSi_2$/Si(001) and $CoSi_2$/Si(001) structures, respectively, compared to 30 meV/Å^2 and 61 meV/Å^2 for the sevenfold-R $NiSi_2$/Si(001) and $CoSi_2$/Si(001) structures. For convenience of comparison, the difference in formation energy, ΔE_{form}, with the energy of sevenfold-R as a reference, normalized over a 2×2 unit, is listed in Table I. Results of Yu *et al.*[8] are also given in brackets in Table I. The formation energy of the sixfold interface is 1.231 eV lower than that of the eightfold for the $NiSi_2$/Si system, while the eightfold is more stable than the sixfold by 0.732 eV for the $CoSi_2$/Si system, which are in agreement with the results of previous studies. However, both structures are less stable compared to the sevenfold-R configuration. As expected, our results clearly show that the sevenfold-Z model proposed here has comparable energy as the sevenfold-R model and both of them are energetically stable. For the $NiSi_2$/Si(001) interface, the formation energy of the sevenfold-Z configuration is 17 meV less compared with the sevenfold R, while it is 19 meV higher for $CoSi_2$/Si(001). The differences are about the order of computational accuracy and it can be concluded that the sevenfold-Z and -R configurations are energetically degenerate.

Table II lists the bond lengths between the interface metal atoms and their seven nearest neighboring Si atoms, which are illustrated in Fig. 1. Bonds 1 to 4 refer to the bonding between the interface metal atoms and the Si atoms in the first Si layer on the silicide side, and bonds 5 to 7 refer to the bonding of the interface metal atoms with the Si atoms on the Si side. For the sevenfold-R model, the pair of bonds $B_\perp^1$ (bond 3) and $B_\perp^2$ (bond 4) perpendicular to the dimers is symmetrical, and the bond length is 2.325 Å for $NiSi_2$/Si and 2.344 Å for $CoSi_2$/Si, respectively. The bonds $B_\parallel^1$ (bond 1) and $B_\parallel^2$ (bond 2) parallel to the dimers are unsymmetrical due to the formation of Si dimers on one side of the metal interface. The two additional Si atoms between the adjacent metal atoms and the formation of the Si dimer induce compression in the vicinity. This causes the elongation of $B_\parallel^2$ and relative contraction of $B_\parallel^1$. The difference between these two bonds is 0.016 Å for $NiSi_2$/Si and 0.030 Å for $CoSi_2$/Si, respectively. In the proposed sevenfold-Z model, the zigzag distribution of the interface Si atoms on both sides of the metal atoms results in a more uniform stress field. Not only are $B_\perp^1$ and $B_\perp^2$ the same, $B_\parallel^1$ and $B_\parallel^2$ are also identical. Two of the three bonds between the M atoms and their three Si neighbors in the Si side, B_{MD}^1 (bond 5) and B_{MD}^2 (bond 6), are

TABLE II. Bond length (Å) between interface metal atoms and their neighboring Si atoms for sevenfold-R and –Z configurations. Refer to Fig. 1 for labels of the bonds.

	$NiSi_2$/Si		$CoSi_2$/Si	
Bond	Sevenfold R	Sevenfold Z	Sevenfold R	Sevenfold Z
$B_\parallel^1$ (1)	2.295	2.304	2.307	2.327
$B_\parallel^2$ (2)	2.311	2.303	2.337	2.327
$B_\perp^1$ (3)	2.325	2.329	2.344	2.343
$B_\perp^2$ (4)	2.325	2.328	2.344	2.343
B_{MD}^1 (5)	2.365	2.370	2.335	2.336
B_{MD}^2 (6)	2.364	2.368	2.337	2.336
B_{MS} (7)	2.371	2.375	2.340	2.361

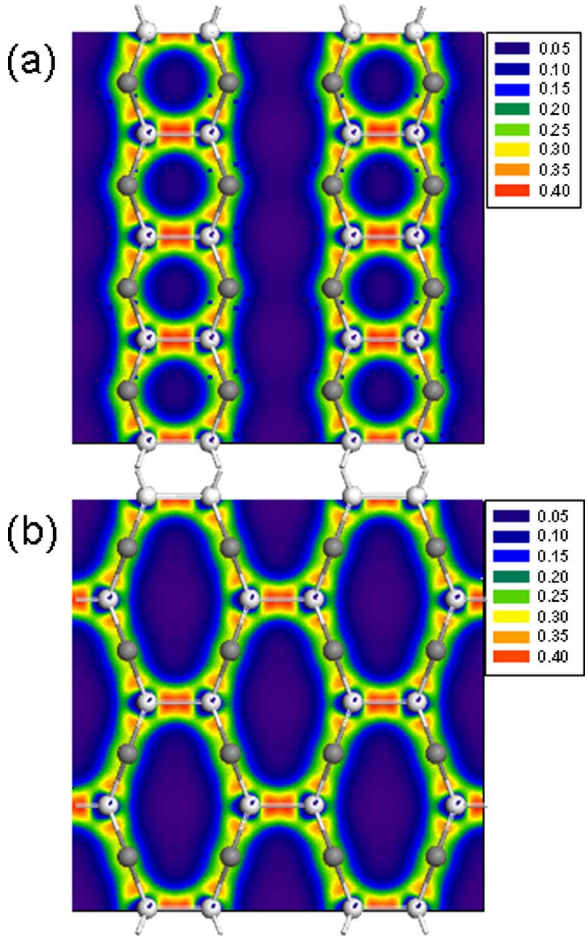

FIG. 3. (Color online) Contour plots of valence electron charge density (electron/Å^3) at the Si-dimer interface plane for (a) sevenfold-R model and (b) sevenfold-Z model, overlaid by atomic structures at the interface plane with Si atoms (light sphere) and projected M atoms (dark ball) for easy reference.

not affected by the configuration of the Si dimers. For the $CoSi_2$/Si interface, the remaining bond between the metal and its Si neighbor, B_{MS} (bond 7), in sevenfold Z is 0.02 Å longer than that in sevenfold R, while it is comparable for both configurations for $NiSi_2$/Si interface. For $NiSi_2$/Si(001), the interatomic-plane distances calculated with both sevenfold reconstructed interface models are in good agreement with the results of the scanning transmission electron microscopy (STEM) obtained by Falke *et al.*[11]

In the work of Falke *et al.*, two different variants of the interface (variant 1 and variant 2) were observed. Compared to variant 2, the interface Si plane in variant 1 is shifted by a quarter of the lattice constant with respect to the position of the outmost Ni layer in silicides. It was assumed that these two variants are orthogonal projections of the 2×1 reconstructed structure, which was classified as the sevenfold-R model. However, it was found that the contrast of the dimerized Si atoms in variant 2 appears relatively blurred, and it was speculated that this is due to a shift of the dimer rows, which cannot be distinguished experimentally. Our sevenfold-Z model gives a good explanation to the experimental results. As shown in Figs. 1(a) and 1(b), the sevenfold-R and sevenfold-Z models have exactly the same projection on the $\langle 1\bar{1}0\rangle$ direction. Considering the comparable interface formation energy and atomic plane distances, it is highly possible that both row configuration and zigzagged configuration coexist for the interface Si dimers, and the interface configuration in variant 2 could be a mixture of the sevenfold-R and sevenfold-Z models. As a result, the STEM image of variant 1 on the $\langle 1\bar{1}0\rangle$ direction is clear because both interface structures produce the same projection, but the image in variant 2 is blur due to the random distribution of the two Si dimer configurations.

Figure 3 shows contour graphs of the valence electron charge density along the interface Si dimer planes of 2×2 sevenfold-R and -Z models. The atomic structures at the interface plane with Si atoms (white sphere) and projected M atoms (dark ball) are overlaid on the contour graph for easy reference. The local electronic structures are the same for the two models although the zigzag Si dimers have a slightly shorter bond length compared to the row dimers. For $NiSi_2$/Si, the Si-Si dimer bond of the sevenfold-Z interface is 0.003 Å shorter than that of the sevenfold R, and the difference is 0.005 Å for $CoSi_2$/Si. Due to the zigzag arrangement, it is noted that the electron charge distribution shows higher symmetry in the sevenfold-Z configuration than that in the sevenfold R. Atomic structure and interface bonding at the metal-semiconductor interface have been proven to be primary mechanisms of the Schottky barrier height (SBH) formation by both experimental and computational results.[20,21] Based on results of our calculations, the sevenfold-R and -Z models are energetically degenerate, indicating that the two types of interface structures can form simultaneously. However, since the two interface configurations are different in terms of dimer bonding direction and length, stacking fault can be easily induced to degrade the interface quality of the heterostructure. The SBH is expected to be affected.

In conclusion, we propose a model for the MSi_2/Si interface, the sevenfold-Z model with a zigzag Si dimer arrangement at the interface, which is based on the existing sevenfold-R model with a row Si dimer arrangement. Results of first-principles electronic structure calculations indicate that this model is equally possible as the sevenfold-R model with comparable interface formation energy and interatomic-plane spacing. The possible coexistence of the sevenfold-Z and the sevenfold-R models explains the clear image in one direction and the blurred Si dimer image in the perpendicular direction observed in the earlier STEM study.

*Electronic address: phyfyp@nus.edu.sg

[1] K. N. Tu, E. I. Alessandrini, W. K. Chu, H. Krautle, and J. W. Mayer, Jpn. J. Appl. Phys., Suppl. **2**, Pt. 1, 669 (1974).
[2] R. T. Tung, J. M. Gibson, and J. M. Poate, Phys. Rev. Lett. **50**, 429 (1983).
[3] W. S. Yang, F. Jona, and P. M. Marcus, Phys. Rev. B **28**, 7377 (1983).
[4] D. R. Hamann and L. F. Mattheiss, Phys. Rev. Lett. **54**, 2517 (1985).
[5] R. T. Tung, J. C. Bean, J. M. Gibson, J. M. Poate, and D. C. Jacobson, Appl. Phys. Lett. **40**, 648 (1982).
[6] L. J. Chen, J. W. Mayer, and K. N. Tu, Thin Solid Films **93**, 137 (1982).
[7] D. Cherns, C. J. D. Hetherington, and C. J. Humphreys, Philos. Mag. A **49**, 165 (1984).
[8] B. D. Yu, Y. Miyamoto, O. Sugino, A. Sakai, T. Sasaki, and T. Ohno, J. Vac. Sci. Technol. B **19**, 1180 (2001).
[9] D. Loretto, J. M. Gibson, and S. M. Yalisove, Phys. Rev. Lett. **63**, 298 (1989).
[10] C. W. T. Bulle-Lieuwma, A. E. de Jong, and D. E. W. Vandenhoudt, Philos. Mag. A **64**, 255 (1991).
[11] U. Falke, A. Bleloch, M. Falke, and S. Teichert, Phys. Rev. Lett. **92**, 116103 (2004).
[12] Y. Tu and J. Tersoff, Phys. Rev. Lett. **84**, 4393 (2000).
[13] P. Hohenberg and W. Kohn, Phys. Rev. **136**, 864 (1964).
[14] G. Kresse and J. Hafner, Phys. Rev. B **47**, R558 (1993); **48**, 13115 (1993); G. Kresse and J. Furthmuller, Comput. Mater. Sci. **6**, 15 (1996); Phys. Rev. B **54**, 11169 (1996).
[15] D. Vanderbilt, Phys. Rev. B **41**, R7892 (1990).
[16] J. P. Perdew, J. A. Chevary, S. H. Vosko, K. A. Jackson, M. R. Pederson, D. J. Singh, and C. Fiolhais, Phys. Rev. B **46**, 6671 (1992).
[17] H. J. Monkhorst and J. D. Pack, Phys. Rev. B **13**, 5188 (1976).
[18] P. Villars and L. D. Calvert, *Pearson's Handbook of Crystallographic Data for Intermetallic Phases* (American Society for Metals, Metals Park, OH, 1985).
[19] R. E. Cohen, O. Glseren, and R. J. Hemley, Am. Mineral. **85**, 338 (2000).
[20] R. T. Tung, Phys. Rev. Lett. **84**, 6078 (2000).
[21] H. Fujitani and S. Asano, Phys. Rev. B **42**, 1696 (1990).